Nucleation and Particle Growth Processes Involved in the Preparation of Silica-Supported Nickel Materials by a Two-Step Procedure

Michel Che, Zheng Xing Cheng, and Catherine Louis*

Contribution from the Laboratoire de Réactivité de Surface, URA 1106 CNRS, Université Pierre et Marie Curie, 4 place Jussieu, 75252 Paris Cedex 05, France

Received December 1, 1993[⊗]

Abstract: A new method of preparation of silica-supported nickel materials makes possible the control of the particle size of metallic nickel in the range 20−60 Å and in particular the obtention of decreasing particle size for increasing metal content. The preparation involves a two-step procedure: nickel in strong interaction with the support is deposited first, then nickel in weak interaction. After temperature-programmed reduction up to 700 °C, metal nickel particles are obtained whose size depends on the respective amounts of nickel deposited at each step of preparation. The average particle size is always smaller and the size distribution narrower than those of samples prepared by classical impregnation. This preparation method involves an easy to carry out procedure: (i) nickel in strong interaction is obtained by impregnation of nickel nitrate followed by water-washing or by ion-exchange followed by calcination; (ii) nickel in weak interaction is obtained by impregnation. It is shown that a mechanism of particle growth on the nickel nuclei is responsible for the changes in particle size. It takes place after impregnation during the drying step at 90 °C via condensation reactions between the two types of nickel. Nickel in strong interaction, identified as phyllosilicates or as grafted nickel depending on the preparation conditions, acts as nucleation sites for the particle growth arising from nickel in weak interaction. During drying in air at 90 °C, impregnated nickel nitrate transforms into a basic nitrate whose OH groups can react either with those in phyllosilicates or with H_2O in the coordination sphere of grafted nickel.

Introduction

Owing to the rapid development of material science and to the important need in advanced composite materials, investigations on thermodynamic and structural properties of oxide−metal bonding and interfaces have been extensive in recent years. Progress in this field has been reviewed.[1−3] Studies dealing with characterization, properties, and preparation of small metal particles and thin solid films of metals on oxide surfaces are of direct relevance to fields such as metallurgy, electronics (miniaturization), energetics, optics (optical coatings), ceramic bonding, decorative applications, surface science, and heterogeneous catalysis. Despite the importance of these applications, the understanding of the nature of the chemical bonding involved at solid−solid interfaces and of the phenomena which control the properties of the deposited metallic phase is still very coarse. Even in model systems, it is recognized that the nature of the surface defects acting as preferred nucleation sites for the growth of metal particles is not known for any planar support material.[4a]

Attempts have been made to prepare in a controlled way metal particles deposited on oxide supports (i) directly by metal vapor condensation techniques in ultrahigh vacuum equipment,[4] (ii) by decomposition of organometallic clusters or complexes,[5] and (iii) by solvated metal atom dispersion techniques.[6]

Another interesting attempt is to deposit metal precursors in an oxidated state and reduce them in a further step. A way to limit the metal particle size was proposed by Yermakov.[7] The introduction of a nonreducible second-transition metal (Mo or W) in the preparation of silica-supported platinum inhibits the undesired agglomeration process by attracting the noble metal Pt cluster to the coordination sphere of the added ions, leading to smaller particles. According to the author, the reduced transition metal would be "chemically anchored" to the support through partially reduced or unreduced ions of the other transition metal. In other words, the less reducible metal acts as an anchoring site for the more reducible metal.

The same type of phenomenon was observed by Klabunde et al. in EXAFS[8a] and XPS studies[8b] of Co−Mn-supported catalysts prepared by using solvated metal atom dispersion techniques. They found that toluene-solvated manganese atoms react with surface OH groups before cobalt atoms:

$$\text{toluene}-\text{Mn}-\text{toluene} + 2{\equiv}\text{SiOH} \rightarrow (\equiv\text{SiO})_2\text{Mn}^{2+} + \text{H}_2 + 2\text{toluene}$$

This is consistent with the fact that manganese is more oxophilic than cobalt. Then, the resultant manganese oxide surface species serve as nucleation sites for cobalt atoms. In the same way,

[⊗] Abstract published in *Advance ACS Abstracts*, January 15, 1995.

(1) Stevenson, S. A.; Dumesic, J. A.; Baker, R. T. K.; Ruckenstein, E. *Metal-Support Interactions in Catalysis, Sintering, and Redispersion*; Van Nostrand: New York, 1989.

(2) Haller, G. A.; Resasco, D. E. *Adv. Catal.* **1989**, *36*, 173−235.

(3) Dufour, L.-C.; Perdereau, M. *Surfaces and Interfaces of Ceramics Materials*; Dufour, L.-C., Nowotny, J., Eds.; Kluwer Academic Publishers: Dordrecht, The Netherlands, 1989; pp 419−448.

(4) (a) Poppa, H. *Catal. Rev.−Sci. Eng.* **1993**, *35*, 359−398. (b) Masson, A.; Bellamy, B.; Hadj Romdhane, Y.; Che, M.; Roulet, H.; Dufour, G. *Surf. Sci.* **1986**, *173*, 479−497. (c) Takasu, Y.; Akimura, T.; Kasahara, K.; Matsuda, Y. *J. Am. Chem. Soc.* **1982**, *104*, 5249−5250.

(5) (a) Zhang, Z.; Suib, S. L.; Zhang, Y. D.; Hines, W. A.; Budnick, J. I. *J. Am. Chem. Soc.* **1988**, *110*, 5569−5571. (b) Schmid, G.; Harms, M.; Malm, J.-O.; Bovin, J.-O.; van Ruitenbeck, J.; Zandbergen, H. W.; Fu, W. T. *J. Am. Chem. Soc.* **1993**, *115*, 2046−2048.

(6) (a) Woo, S. I.; Gobber, J.; Ozin, G. A. *J. Mol. Catal.* **1989**, *52*, 241−252. (b) Klabunde, K. J.; Yong, Y.-X.; Tan, B.-J. *Chem. Mater.* **1991**, *3*, 30−39.

(7) Yermakov, Y. I. *Catal. Rev.−Sci. Eng.* **1976**, *13*, 77−120.

(8) (a) Tan, B.-J.; Klabunde, K. J.; Tanaka, T.; Kanai, H., Yoshida, S. *J. Am. Chem. Soc.* **1988**, *110*, 5951−5958. (b) Tan, B.-J.; Klabunde, K. J.; Sherwood, M. A. *J. Am. Chem. Soc.* **1991**, *113*, 855−861. (c) Delafosse, D. *J. Chim. Phys.* **1986**, *83*, 791−799.

0002-7863/95/1517-2008$09.00/0

Ce^{3+} ions have been shown to act as anchoring sites of Ni particles encaged in zeolites.[8c]

Sachtler et al.[9] also suggested that, in zeolites, the same phenomenon was responsible for the formation of small metal particles when Fe and Cr were respectively added to Pt and Rh exchanged in Y zeolite. Fe or Cr ions, electrostatically bound to the zeolite oxygen anions, act as anchoring sites and inhibit the migration of atoms or small particles of Rh or Pt through the zeolite channels during reduction and therefore result in a lower average particle size. However, in the Co−Pd/Y zeolite system, Moller and Bein[10] showed that the higher dispersion of Pd particles was not associated with chemical anchoring but with a change in cation distribution: the Co ions are preferentially located in the sodalite cages and force the palladium cations into the supercages. For the Fe−Pd/Y system, the situation is again different since the iron does not influence the Pd particle size.[11] These results show that the interplay of metals is not easily predictable and strongly depends on the chemistry of each constituent. In addition, the problem is complicated in zeolites by the fact that ion migration can occur even at low temperature,[12] mainly because of the different Coulomb interaction of metal cations with the negatively charged zeolite framework in the different cages.[13] This phenomenon is less likely to occur with supports such as silica or alumina because of the absence of cages.

In the Rh−Fe, Pt−Fe, and Pd−Fe bimetallic catalysts prepared by impregnation with mixed carbonyl clusters onto silica, the Fe^{III} ions were reported to be located at the interface between the support and the Rh^0, Pt^0, or Pd^0 clusters, respectively, and to be involved in Fe−O−support bonding in the metal−support interface, playing the role of anchoring sites for Rh, Pt, or Pd particles, respectively.[14] A similar interaction was found by Sinfelt et al.[15] for Sn^{II} and Pt^0 supported on alumina. For a monometallic system, such as Mo/γ-Al_2O_3, obtained from the activation of $Mo(CO)_6/\gamma$-Al_2O_3 by hydrogen at 650 °C, Bowman and Burwell[16] proposed that Mo^{II} is first formed on the surface of the alumina by reaction of AlOH with Mo^0 obtained from $Mo(CO)_6$ decomposition:

$$Mo^0 + 2AlOH \rightarrow Mo^{II} + 2AlO^- + H_2$$

and that further Mo^0 collects on the top of Mo^{II} to form clusters. For the Ni/SiO_2 system, the anchoring of the metal particles onto the support was found to occur via Ni^I or/and Ni^{II} ions located at the metal−support interface.[17] For Pt/SiO_2 and Pt/Al_2O_3, Huizinga and Prins[18] demonstrated that Pt^I ions are in contact with platinum metal particles and are located at the metal−support interface. Koningsberger et al.[19] showed by extended X-ray absorption fine structure (EXAFS) that the metals in clusters at the metal−oxide support interface may be sufficiently polarized to bear slight but significant positive charges and to bond to the oxygen of the support, helping to anchor the metal clusters and stabilize their dispersion. In the case of Pt/TiO_2 catalysts representative of systems with metal particles supported on reducible oxides and exhibiting the strong metal support interaction (SMSI) effect,[20] it is generally agreed[2] that Ti interacting with metal particles is a cation of lower oxidation state than in TiO_2, i.e. Ti^{III} or Ti^{II}. In addition, it has been claimed that direct metal−Ti^{III} or −Ti^{II} bonding occurs in the Rh/TiO_2 system.[21]

These sequences of chemical bonds, either ionic or covalent in character, between the support and the metal are also called "chemical glue" in the literature.[22−28] From the survey given above and as studied earlier,[29] it appears that the chemical glues can be formed by exposed metal ions either in framework positions or in extraframework positions. Exposed ions are probably not the only chemical species which can act as anchoring sites. Thus, it has been observed that color centers produced by UV irradiation of oxides such as $SrTiO_3$, Al_2O_3,[30] and CeO_2[31] mediate catalytic activity for electroless plating of metal from solutions containing Cu, Ni,[30] or Pd[31] ions.

According to Labadz and Lowell,[32] the positive charge borne by the metal at the interface arises from an electron transfer between the metal and the surface of the oxide insulator. Their results confirm those of Hays and Donald,[33] i.e. the states on (or near) the surface oxide can readily exchange electrons with the contacting metal but are isolated from electron states in the bulk of the oxide. There have been several theoretical studies performed on the adhesion of metals on oxides or ceramics[23,25−27] with emphasis either on the physical interaction or on the chemical one.

As far as chemical interaction is concerned, the likely existence of this "chemical glue" has prompted us to prepare silica-supported nickel particles using a two-step procedure. Its principle is based on the deposition of nickel ions in strong

(9) (a) Tzou, M. S.; Jiang, H. J.; Sachtler, W. M. H. *Appl. Catal.* **1986**, *20*, 231−238. (b) Tzou, M. S.; Teo, B. K.; Sachtler, W. M. H. *Langmuir* **1986**, *2*, 773−776.

(10) Moller, K.; Bein, T. *Zeolites: Facts, Figures, Future*; Jacobs, P. A., van Santen, R. A., Eds.; Elsevier Science Publishers: Amsterdam, 1989; pp 985−994.

(11) Moller, K.; Bein, T. *J. Phys. Chem.* **1990**, *94*, 845−853.

(12) Olivier, D.; Richard, M.; Che, M. *Chem. Phys. Lett.* **1978**, *60*, 77−80.

(13) Homeyer, S. T.; Sachtler, W. M. H. *Zeolites: Facts, Figures, Future*; Jacobs, P. A., van Santen, R. A., Eds.; Elsevier Science Publishers: Amsterdam, 1989; pp 975−984.

(14) (a) Ichikawa, M.; Fukushima, T.; Yokoyama, T.; Kosugi, N.; Kuroda, H. *J. Phys. Chem.* **1986**, *90*, 1222−1224. (b) Fukuoka, A.; Ichikawa, M.; Hriljac, J. A.; Shriver, D. F. *Inorg. Chem.* **1987**, *26*, 3643−3645. (c) Fukuoka, A.; Kimura, T.; Ichikawa, M. *J. Chem. Soc., Chem. Commun.* **1988**, 428−430. (d) Fukuoka, A.; Kimura, T.; Kosugi, N.; Kuroda, H.; Minai, Y.; Sakai, Y.; Tominaga, T.; Ichikawa, M. J. *J. Catal.* **1990**, *126*, 434−450.

(15) Meitzner, G.; Via, G. H.; Lytle, F. W.; Fung, S. C.; Sinfelt, J. H. *J. Phys. Chem.* **1988**, *92*, 2925−2932.

(16) (a) Bowman, R. G.; Burwell, R. L. *J. Catal.* **1980**, *63*, 463−475. (b) Nakamura, R.-I.; Bowman, R. G.; Burwell, R. L. *J. Am. Chem. Soc.* **1981**, *103*, 673−674.

(17) Bonneviot, L.; Che, M.; Olivier, D.; Martin, G. A.; Freund, E. *J. Phys. Chem.* **1986**, *90*, 2112−2117.

(18) Huizinga, T.; Prins, R. *J. Phys. Chem.* **1983**, *87*, 173−176

(19) (a) Koningsberger, D. C.; Gates, B. C. *Catal. Lett.* **1992**, *14*, 271−277. (b) Van Zon, F. B. M.; Maloney, S. D.; Gates, B. C.; Koningsberger, D. C. *J. Am. Chem. Soc.* **1993**, *115*, 10317−10326.

(20) Tauster, S. J.; Fung, S. C.; Garten, R. L. *J. Am. Chem. Soc.* **1978**, *100*, 170−175.

(21) Sakelson, S.; Mc Millan, M.; Haller, G. L. *J. Phys. Chem.* **1986**, *90*, 1733−1739.

(22) Coenen, J. W. E. *Preparation of Catalysts II*; Poncelet, G., Grange, P., Jacobs, P. A., Eds.; Elsevier: Amsterdam, 1979; pp 89−108.

(23) Horsley, J. A. *J. Am. Chem. Soc.* **1979**, *101*, 2870−2874.

(24) Bond, G. C. *Surf. Sci.* **1985**, *156*, 966−981.

(25) Alemany, P.; Boorse, R. S.; Burlitch, J. M.; Hoffman, R. *J. Phys. Chem.* **1993**, *97*, 8464−8475.

(26) Boorse, R. S.; Alemany, P.; Burlitch, J. M.; Hoffman, R. *Chem. Mater.* **1993**, *5*, 459−464.

(27) Che, M.; Masure, D.; Chaquin, P *J. Phys. Chem.* **1993**, *97*, 9022−9027.

(28) Che, M.; Bennett, C. O. *Adv. Catal.* **1989**, *36*, 55−172.

(29) Che, M. *Proceedings of the 10th International Congress on Catalysis*, Budapest, July 19−24, 1992; Studies in Surface Science and Catalysis; Guczi, L., Solymosi, F., Tétényi, P., Eds.; Elsevier Science Publishers: Amsterdam, and Acadêmiai Kiado: Budapest, 1993; Vol. A, pp 31−68.

(30) Shafeev, G. A. *Adv. Mater. Opt. Electron.* **1993**, *2*, 183−189.

(31) Bensalem, A.; Shafeev, G. A.; Bozon-Verduraz, F. *Catal. Lett.* **1993**, *18*, 165−171.

(32) Labadz, A. F.; Lowell, J. *J. Phys. D: Appl. Phys.* **1991**, *24*, 1416−1421.

(33) Hays, D.; Donald, D. K. *Annual Report of the Conference on Electrical Insulation and Dielectric Phenomena*; National Academy of Sciences: Washington, DC, 1972; pp 74−80.

interaction with silica which will act as "chemical glue", followed by impregnation of a nickel salt, forming a "nickel reservoir" in weak interaction with the support.

In a previous work,[34] we have reported on the evidence of a growth mechanism of nickel particles onto the "chemical glue", i.e. on "nickel nuclei", after impregnation. Indeed, after thermal reduction under hydrogen, it has been possible to obtain nickel metal particles with average diameters between 20 and 60 Å, depending on the relative amounts of "nickel nuclei" and "nickel reservoir".

However, several questions remained unanswered: (i) At which step of preparation or reduction does the nickel particle growth occur, and what kind of nickel leads to the formation of particles, nickel in the metallic or oxidized state? (ii) What is the mechanism of growth of the nickel particles?

The goal of the present work is an attempt to answer these questions and to document the approach given in the previous paper[34] by new results.

Experimental Section

(1) Sample Preparation. (a) Sample Preparation by a Two-Step Procedure. Step 1: Preparation of "Nickel Nuclei". (1) By cation-exchange with hexaamminenickel(II), $[Ni(NH_3)_6]^{2+}$. The samples were prepared from a solution of ammonium nitrate (1 mol/L) to which nickel nitrate was added in order to obtain solutions with different concentrations (0.05, 0.025, and 0.001 mol/L). The solution pH was adjusted to 9.8 by bubbling gaseous NH_3. At this pH, the main nickel species is $[Ni(NH_3)_6]^{2+}$.[35] This solution (70 cm^3) was added to 5 g of silica. The suspensions were continuously stirred at 25 °C in a thermostated vessel for 24 h. Then, they were filtered and the samples were washed with a solution of ammonium nitrate (1 mol/L) at pH 9.8. The samples were dried for 24 h at 90 °C and then calcined in air at 500 °C for 2 h in order to decompose nitrate and hexaamminenickel(II). The samples are hereafter referred to as $ENi_{NH_3}x/500$, where x is the nickel loading expressed in wt % of nickel per gram of dehydrated silica and 500 indicates the calcination temperature.

(2) By cation-exchange with tris(ethylenediamine)nickel(II), $[Ni(en)_3]^{2+}$. The samples were prepared from solutions of $[Ni(en)_3](NO_3)_2$ (0.5, 0.13, and 0.05 mol/L). These solutions were obtained with a mixture of nickel nitrate solutions and ethylenediamine. The concentration ratio [en]/[Ni^{II}] was higher than 3 in order to form the $[Ni(en)_3]^{2+}$ complex (pH ≈ 12). The solution (80 cm^3) was added to 5 g of silica. The suspensions were continuously stirred at 25 °C in a thermostated vessel for 48 h. Then, they were filtered and the samples were washed with a 0.24 M ethylenediamine solution at pH 12. The samples were dried at 90 °C for 24 h and then calcined in air at 600 °C for 2 h in order to decompose nitrate and (ethylenediamine)nickel(II). The samples $[Ni(en)_3]^{2+}/SiO_2$ are hereafter referred to as $ENi_{en}x/600$, where x is the nickel loading, and 600, the calcination temperature.

(3) By water-washing of impregnated Ni/SiO_2 samples. The impregnation of silica with nickel was performed by incipient wetness impregnation (2 mL/g) with an aqueous solution of nickel nitrate (3.4 mol/L; beyond this concentration, the solution is saturated). The mixture was kept at room temperature for 2 h before drying at 90 °C for 18 h. The nickel loading is 47 wt %. The sample was then thoroughly washed with water at room temperature through a Büchner until the water remained colorless. After water-washing, the Ni loading is less than 1% of the initial one. The amount of nonsoluble Ni was increased by performing several cycles of impregnation (47 wt % of Ni)−drying (90 °C/18 h)−water-washing−drying (90 °C/18 h). The water-washed impregnated samples are hereafter referred to as IWNix.

Step 2: Impregnation of the "Nickel Reservoir". The "nickel reservoir" was obtained by impregnation of silica containing "nickel nuclei", with different concentrations of nickel nitrate according to the method described above. The impregnating volume was 1.5 mL/g for the water-washed samples and 1 mL/g for the exchanged samples.[36]

(34) Cheng, Z. X.; Louis, C.; Che, M. *Z. Phys. D* **1991**, *20*, 445−448.
(35) Clause, O. Doctoral Thesis, Université Pierre et Marie Curie, Paris, 1989.

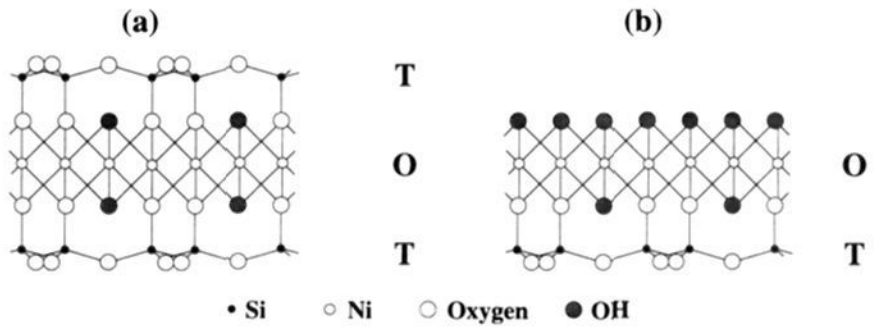

Figure 1. Projection on the *bc* plane of (a) a TOT layer of 2:1 nickel phyllosilicate and (b) a TO layer of 1:1 nickel phyllosilicate (ref 39).

These samples are referred to as IWNi+INi, $ENi_{NH_3}/500$+INi, and $ENi_{en}/600$+INi, depending on the nature of the nuclei.

(b) Reference Samples. The reference samples for the IWNi+INi samples, referred to as INi, were prepared by impregnation as described above. The reference samples of the $ENi_{NH_3}/500$+INi and $ENi_{en}/600$+INi samples whose "nickel nuclei" were prepared in basic medium and under magnetic stirring, and then calcined, were obtained by impregnation of silicas previously submitted to the same conditions of exchange except for the presence of nickel, and then calcined. They are called $NH_3-SiO_2/500$+INi and en−$SiO_2/600$+INi.

All the samples were prepared with silica Spherosil XOA400 (Rhône Poulenc, France, S_{BET} = 400 m^2/g, pore volume = 1.25 cm^3/g, average pore diameter = 80 Å).

(2) Techniques. Chemical analyses of nickel were performed in the Center of Chemical Analysis of the CNRS (Vernaison, France).

The XRD spectra were carried out on a Siemens diffractometer (D500). The phase identifications were performed by comparison with the tabulated JCPDS d-spacing files.

UV−visible−near-IR spectra were recorded on a Beckman 5270 reflectance spectrometer equipped with an integration sphere and a double monochromator. $BaSO_4$ was used as the reference.

EXAFS measurements at the absorption edge of Ni were performed at the LURE Radiation Synchrotron Facility (EXAFS I) using the X-ray beam emitted by the DCI storage ring (positron energy = 1.85 GeV, ring current = 300 mA). The spectra were recorded in transmission mode at room temperature using two air-filled ionization chambers. The energy was scanned with 2 eV steps from 8200 to 9200 eV (K absorption edge of Ni = 8331 eV), using a channel-cut single crystal of silicon as the monochromator. EXAFS measurements were carried out three times for each sample. The absorption variation through the edge $\Delta(\mu x)$ was at least 0.5.

The analyses of the EXAFS spectra were performed by following standard procedures for background removal, extraction of the EXAFS signal, and normalization to the edge absorption. Fourier transforms were obtained after multiplication of the EXAFS signal by a factor k^3, using the same Hanning window for the references and the investigated systems. Data treatment was performed with the software "EXAFS pour le Mac".[37]

Amplitude and phase functions for O, Ni, and Si backscatterers were experimentally obtained from the spectra of well-crystallized $Ni(OH)_2$ and Ni-doped $Mg(OH)_2$ (Ni:$Mg(OH)_2$). The latter compound was considered as a reference for Si backscatterers because the masses of Si and Mg are very close.[38] The distances, numbers of backscatterers, and Debye−Waller factors ($\Delta\sigma^2$) are gathered in Table 1. Two synthetic nickel silicates with layer structures, a 2:1 phyllosilicate ($Ni_3Si_4O_{10}(OH)_2$, also called talc) and a 1:1 phyllosilicate ($Ni_3Si_2O_5(OH)_4$, also called nepouite)[39] (Figure 1), kindly supplied by A. Decarreau (Laboratoire de Pétrologie de la Surface, University of Poitiers, France), were used as references for the Debye−Waller factor calibration (Figure 2a,b, Table 1).

The samples were reduced by temperature-programmed reduction (TPR), from room temperature to 700 °C, with a heating rate of 7.5

(36) During the preparation by exchange, the use of both a basic solution which attacks silica and a magnetic stirrer caused the grinding of silica, and ground silica requires a lower impregnating volume to be wetted.
(37) (a) Michalowicz, A. Doctoral Thesis, Université Paris XII-Val de Marne, 1990. (b) Michalowicz, A. EXAFS Pour le Mac. In *Logiciels pour la Chimie*; Société Française de Chimie: Paris, 1991; p 102.
(38) Clause, O.; Kermarec, M.; Bonneviot, L.; Villain, F.; Che, M. *J. Am. Chem. Soc.* **1992**, *114*, 4709−4717.

Table 1. Structural Parameters of the Ni References and of the $ENi_{NH_3}2.7/500$ and $ENi_{en}2.4/600$ Samples Determined by EXAFS at the Ni K-Edge of the Second Shell[a]

samples	shell atom	no. of backscatterers	distance (Å)	$\Delta\sigma^2$ (Å^2)	Q	refs
$Ni(OH)_2$	Ni	6.0	3.13			40
$Ni:Mg(OH)_2$	Mg	6.0	3.14			40
1:1 phyllosilicate	Ni	6.0	3.09	0	7.8×10^{-3}	this work
	Si	2.5	3.30	−0.0017		
2:1 phyllosilicate	Ni	6.0	3.07	−0.0017	7.5×10^{-3}	this work
	Si	5.0	3.32	0		
$ENi_{NH_3}2.7/500$	Ni	5.9	3.07	0.0019	7.1×10^{-3}	this work
	Si	5.0	3.31	0		
$ENi_{en}2.4/600$	Ni	1.5	3.08	0.0019	5.1×10^{-3}	this work
	Si	3.3	3.27	0		

[a] The best fits are obtained by minimizing the agreement factor Q (least squares minimization algorithm). $\Delta\sigma^2$ is equal to $(\Delta\sigma^2_{(sample)} - \Delta\sigma^2_{(ref)})$. The electron mean free path, Γ, is equal to 1.0 Å^{-2} for all the samples.

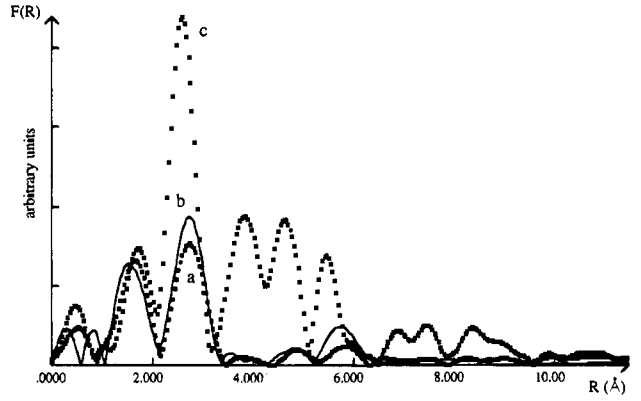

Figure 2. Fourier transform (k^3-weighted, without phase correction) of experimental EXAFS data of (a) 1:1 nickel phyllosilicate, (b) 2:1 nickel phyllosilicate, and (c) NiO.

°C/min, under 5% H_2 in argon (25 cm^3/min) at atmospheric pressure. The intensities of the TPR profiles are expressed in arbitrary units and are not comparable since both the sample weight and the attenuation of the catharometer detector may be different. It was checked separately[41] with quantitative TPR equipment that nickel can be considered as fully reduced when the TPR profiles of Ni/SiO_2 samples return to the baseline.

The nickel particle sizes resulting from the reduction by TPR up to 700 °C were measured from electron micrographs obtained by transmission electron microscopy (TEM, JEOL 100CXII UHR). The average particle diameter $\bar{d}$ was calculated from the following formula: $\bar{d} = \sum n_i d_i / \sum n_i$, where n_i is the number of particles of diameter d_i and $\sum n_i \approx 300$. The detection limits are 10 and 15 Å for metal and oxide nickel particles supported on silica, respectively. A measurement of the concentration of particles (N_s) was obtained from the number of particles per square centimeter of silica on the micrographs (magnification = 160 000). It may be noted that the measured surface area does not correspond to the real silica surface since ground particles of silica always possess a given thickness. However, the N_s values can allow the comparison of the particle concentrations in different samples.

Results and Discussion

(1) Characterization of the Reference Impregnated Samples. The TPR profiles of the three types of Ni/SiO_2 reference samples, INi, NH_3−SiO_2/500+INi, and en−SiO_2/600+INi, are the same regardless of the treatments undergone by the silica

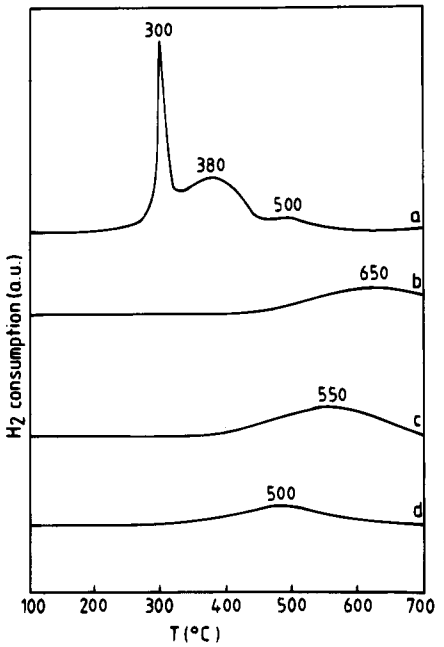

Figure 3. TPR profiles of (a) reference sample: en−SiO_2/600+INi3.0, (b) $ENi_{NH_3}2.7/500$ up to 800 °C, (c) $ENi_{en}2.4/600$, and (d) IWNi0.6.

support and typically look like the one of Figure 3a. They exhibit three peaks at 300, 380, and about 500 °C. In a previous study on impregnated Ni/SiO_2 materials,[42] the first peak at 300 °C was attributed to the decomposition of nickel nitrate into NiO, the second one at 380 °C to the reduction of NiO into Ni^0, and the third one at about 500 °C to the reduction of nickel phyllosilicates formed during preparation. It was found that 80% of the nickel is reduced below 400 °C. This nickel fulfills the conditions so as to be considered as a "nickel reservoir" for the second step of the two-step preparation since most of it is in weak interaction with the silica surface[42] and, thus, will be able to participate to the particle growth.

After TPR up to 700 °C, the average diameter of metal particles measured by TEM is about 65 Å and the size distribution varies between 20 and 150 Å no matter the reference sample and the Ni loading (Table 2). The concentration of particles (N_s), also reported in Table 2, increases with the Ni loading, which is consistent with the constant average particle size.

The similarities in the nickel reducibility (same TPR profile) and the metal particle size of these different samples indicate that the different pretreatments undergone by silica (basic medium and calcination) have no effect on these parameters.

(39) The layers in 1:1 phyllosilicates consist of a brucite-type sheet containing Ni^{II} in octahedral coordination and a sheet containing linked tetrahedral SiO_4 units ions. In 2:1 phyllosilicates, two sheets of linked SiO_4 units sandwich the brucite-type sheets. Bailey, S. W. *Crystal Structure of Clay Minerals and their Diffraction X-Ray Identification*; Brindley, G. W., Brown, G., Eds.; Mineralogical Society: London, 1984; pp 2−6.

(40) Manceau, A.; Calas, G. *Clay Miner.* **1986**, *21*, 341−360.

(41) Burattin, P. Doctoral Thesis, Université Pierre et Marie Curie, Paris, 1994.

(42) Louis, C.; Cheng, Z. X.; Che, M. *J. Phys. Chem.* **1993**, *97*, 5703−5712.

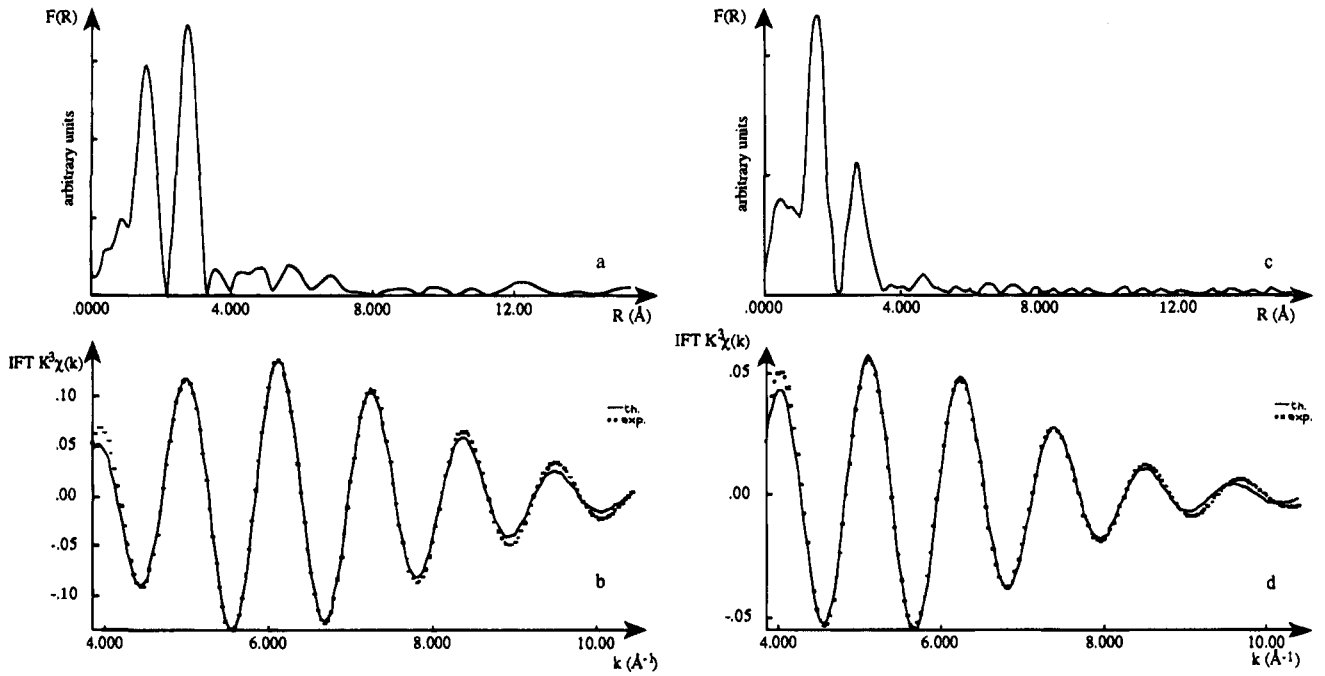

Figure 4. EXAFS spectra of the $ENi_{NH_3}2.7/500$ catalyst: (a) Fourier transform (k^3-weighted, without phase correction) and (b) Fourier filtered inverse spectrum (dots) for the second shell and best simulated spectrum (solid line). EXAFS spectra of the $ENi_{en}2.4/600$ catalyst: (c) Fourier transform (k^3-weighted, without phase correction) and (d) Fourier filtered inverse spectrum (dots) for the second shell and best simulated spectrum (solid line).

Table 2. Characteristics of the Reference Samples: Impregnated Nickel on Pretreated Silicas

ref samples	Ni (wt %)	$\bar{d}$ (Å)	size dist (Å)	N_s (10^{11}/cm^2)
NH_3–SiO_2/500+INi	1.5	66	20–150	0.6
	6.0	65	20–160	2.8
en–SiO_2/600+INi	1.5	66	20–130	0.7
	3.0	69	20–160	1.5
	6.0	66	20–150	2.4
INi	1.5	66	20–140	0.7
	3.5	62	20–150	1.3
	6.1	67	20–160	2.0
	9.2	70	20–150	2.9

Hence, the changes in nickel reducibility and in metal particle size that will be observed after the two-step preparation procedure can be unambiguously attributed to the presence of "nickel nuclei".

It may be noted that, in contrast to our results, Guo et al.[43,44] have observed an influence of the calcination temperature of silica gel, from 400 to 850 °C prior to impregnation, on the nickel metal dispersion. According to the authors,[44] the surface hydroxyl groups of silica gels are of importance for dispersing nickel by wet impregnation and the nickel dispersion does not follow a monotonic dependence on the amount of those surface groups. However, they have not yet elucidated the role of these hydroxyl groups.

(2) Characterization of the "Nickel Nuclei". (a) Characterization of the ENi_{NH_3}/500 Samples. The Fourier transform of the EXAFS spectrum of the $ENi_{NH_3}2.7/500$ sample exhibits two peaks corresponding to the backscatterers and next nearest nickel backscatterers (Figure 4a). The second peak is more intense than the first one, and the spectrum looks like that of nickel phyllosilicates (Figure 2a,b) and not that of NiO (Figure 2c). The simulation of the second peak (Figure 4b) indicates that nickel possesses about six Si atoms and five Ni atoms as next nearest backscatterers with distances Ni···Si and Ni···Ni close to those of the 2:1 phyllosilicate (Table 1, Figure 1a). The presence of phyllosilicates is in good agreement with the results obtained by Clause et al.,[35,38,45] Houalla et al.,[46,47] and Espinos et al.[48] on materials prepared by the same method.

The TPR profile of the $ENi_{NH_3}2.7/500$ sample is composed of a unique broad peak with a maximum temperature at about 650 °C (Figure 3b). This result indicates that nickel, mainly as 2:1 phyllosilicate, is not easily reducible and thus interacts strongly with silica. Figure 3b shows that nickel is not completely reduced at 700 °C. Table 3 shows that the particle sizes after TPR up to 700 °C lie between 10 and 40 Å with an average size smaller than 30 Å.

(b) Characterization of the ENi_{en}/600 Samples. When the ENi_{en}/600 samples were exposed to air at room temperature after calcination, their colors changed from pale pink initially to pale brown, yellow, and then white. In contrast, the ENi_{NH_3}/500 samples remained white under the same conditions. Bonneviot[49] also observed the same changes in color for silica exchanged with hexaamminenickel(II), calcined at 500 °C, evacuated at 700 °C, and then exposed to air. The UV–visible–near-IR diffuse reflectance spectrum of the white ENi_{en}/600 samples exhibits the same absorption bands at 410, 660, and 1160 nm (Figure 5) as in ref 49. They may be also attributed to those of an isolated hexacoordinated grafted nickel species[49] (Figure 6a). Another band observed at 330 nm may correspond to that of a dimer of grafted nickel (Ni^{II}–O–Ni^{II}) according to the same authors[49] (Figure 6b). The absence of bands in the near-IR range at 1530 and 2030 nm due to the N–H vibrations of ethylenediamine indicates that ethylenediamine adsorbed onto the silica surface was decomposed.[50]

(43) Guo, S. L.; Arai, M.; Nishiyama, Y. *Appl. Catal.* **1990**, *65*, 31–44.
(44) Arai, M.; Guo, S. L.; Nishiyama, Y. *J. Catal.* **1992**, *135*, 638–641.
(45) Clause, O.; Bonneviot, L.; Che, M. *J. Catal.* **1992**, *138*, 195–202.
(46) Houalla, M.; Delannay, F.; Matsuura, I.; Delmon, B. *J. Chem. Soc., Faraday Trans. 1* **1980**, *76*, 2128–2141.
(47) Houalla, M. *Preparation of Catalysts III*; Poncelet, G., Grange, P., Jacobs, P. A., Eds.; Elsevier: Amsterdam, 1983; pp 273–320.
(48) Espinos, J. P.; Gonzalez-Elipe, A. R.; Caballero, A.; Garcia, J.; Munuera, G. *J. Catal.* **1992**, *136*, 415–422.
(49) Bonneviot, L. Doctoral Thesis, Université Pierre et Marie Curie, Paris, 1983.

Table 3. Characteristics of Samples Containing "Nickel Nuclei" and "Nickel Reservoir"

nickel nuclei	Ni (wt %)	$\bar{d}$ (Å)	size dist (Å)	N_s (10^{11}/cm^2)	+nickel reservoir	Ni (wt %)	total Ni (wt %)	$\bar{d}$ (Å)	size dist (Å)	N_s (10^{11}/cm^2)
ENi_{NH_3}/500	0.1	<10			ENi_{NH_3}/500+INi	1.5	1.6	68	20−140	0.6
	0.8	24	10−40	4.4		1.5	2.3	45	20−110	4.2
	2.7	26	10−40	11.3		1.5	4.2	28	10−80	11.0
	2.7	26	10−40	11.3		3.0	5.7	46	10−120	10.8
	2.7	26	10−40	11.3		6.0	8.7	54	10−120	9.7
ENi_{en}/600	1.3	<10			ENi_{en}/600+INi	1.5	2.8	31	20−60	6.7
	2.4	18	10−30	11.4		1.5	3.9	19	10−40	11.5
	2.4	18	10−30	11.4		3.0	5.4	30	10−60	11.0
	2.4	18	10−30	11.4		6.0	8.4	41	10−100	10.4
IWNi	(1)[a] 0.6	23	10−30	4.0	IWNi+INi	3.5	4.1	43	20−90	4.0
	(3) 2.3	23	10−40	6.7		3.5	5.8	34	20−80	7.2
	(6) 5.1	17	10−30	10.2		3.5	8.6	26	10−50	9.4
	(6) 5.1	17	10−30	10.2		7.0	12.1	42	20−80	8.6
	(6) 5.1	17	10−30	10.2		9.5	14.6	54	10−120	8.5

[a] Number of cycles of impregnation (47 wt % of Ni)−washing (see the Experimental Section).

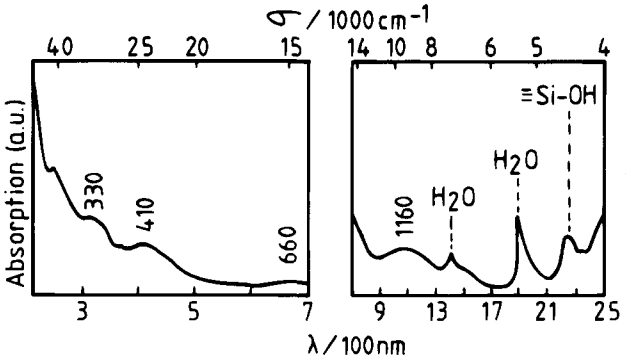

Figure 5. UV−visible−near-IR diffuse reflectance spectra of the ENi_{en}2.4/600 catalyst.

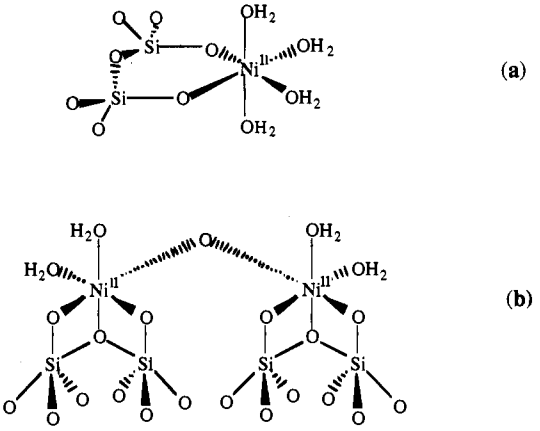

Figure 6. Scheme of (a) an isolated hexacoordinated grafted nickel species and (b) a dimer of grafted nickel (Ni^{II}−O−Ni^{II}) according to ref 49.

The EXAFS Fourier transform of the ENi_{en}2.4/600 sample (Figure 4c) fits neither with that of nickel phyllosilicates (Figure 2a,b) nor with that of NiO (Figure 2c). The simulation of the second peak (Figure 4d) provides a good fit for an average of 1.5 Ni and 3.3 Si backscatterers per Ni (Table 1). This result confirms that obtained by diffuse reflectance spectroscopy: nickel is mainly a mixture of monomers and dimers of grafted nickel (Figure 6).

The TPR profile is composed of a unique broad peak with a maximum temperature at about 550−600 °C (Figure 3c), indicating a low reducibility of nickel as for ENi_{NH_3}2.7/500 (Figure 3b). However, in contrast to the ENi_{NH_3}/500 samples, the ENi_{en}/600 samples are completely reduced at 700 °C.

After TPR of ENi_{en}/600, the metal particles are only observed by TEM for Ni loadings above 2 wt %. The particle sizes vary between 10 and 30 Å with an average diameter of about 18 Å (Table 3).

(c) Characterization of the Water-Washed Ni/SiO_2 Samples, IWNi. In a previous EXAFS study,[42] nickel in the water-washed Ni/SiO_2 samples has been identified as a 1:1 phyllosilicate. Its TPR profile consists only of one broad reduction peak in the 350−650 °C range, with a maximum at about 500 °C (Figure 3d). The average particle diameter after TPR to 700 °C is less than 25 Å with a narrow size distribution (Table 3).

(d) Discussion. After reduction up to 700 °C, the ENi_{NH_3}/500, ENi_{en}/600, and IWNi samples give much smaller particles (less than 30 Å) and narrower size distributions than the reference samples (≈65 Å). When the Ni loading is high enough so as to permit the observation of metal particles by TEM, the average particle size is almost constant for each series of samples and the concentration of particles (N_s) increases with the Ni loading (Table 3).

In addition, all the samples exhibit a unique reduction peak at high temperature, indicating strong interactions between nickel and silica. These nickel species fulfill the conditions required to be considered as "nickel nuclei". However, their nature depends on the conditions of preparation: nickel in the ENi_{en}/600 samples is a grafted Ni^{II} species, whereas that in the IWNi and ENi_{NH_3}/500 samples is engaged in phyllosilicates. These two types of "nickel nuclei" also differ by the fact that grafted Ni is located in an extraframework position whereas nickel of phyllosilicates may be considered as in a framework position.[29]

The nickel reducibility in ENi_{NH_3}/500 samples is found to be lower than in IWNi samples (Figure 3b,d). That should mean that nickel in 2:1 phyllosilicates is less reducible than nickel in 1:1 phyllosilicates, which is in agreement with results reported for unsupported compounds.[51] However, recent studies in our laboratory have shown that TPR is not helpful in confirming the assignment to a type of phyllosilicate. Indeed, the TPR peak position of unsupported phyllosilicates has been shown to be also dependent on the conditions of hydrothermal synthesis[52] (nature of the precursors, temperature, and aging time) which determine the level of impurities[53] and the crystallinity of the

(50) Cheng, Z. X. Doctoral Thesis, Université Pierre et Marie Curie, Paris, 1992.

(51) Wendt, G.; May, M. *Z. Chem.* **1988**, *26*, 177−178.

(52) From a mixture of silica and nickel salt in basic medium under hydrothermal conditions, see: Martin, G. A.; Renouprez, A.; Dalmai-Imelik, G.; Imelik, B. *J. Chim. Phys.* **1970**, *67*, 1149−1160. Mizutami, T.; Fukushima, Y.; Okada, A.; Kamigaito, O. *Bull. Chem. Soc. Jpn.* **1990**, *63*, 2094−2098.

(53) Carriat, J. Y. Doctoral Thesis, Université Pierre et Marie Curie, Paris, 1994.

phyllosilicates.[54] In addition, the assignment to a type of phyllosilicates on the basis of EXAFS is not as straightforward as expected. The attribution of a spectrum to a 1:1 phyllosilicate does not rule out the presence of a small amount of 2:1 phyllosilicate.[55] In addition, the number of Ni and Si backscatterers has been shown to depend strongly on the crystallinity of the phyllosilicate.[53] That reveals the acute problem of the choice of the right references. In summary, we prefer to attribute the nickel in the $ENi_{NH_3}/500$ and IWNi samples to phyllosilicates although the two are obviously different since nickel in the $ENi_{NH_3}/500$ samples is not completely reduced after TPR up to 700 °C, in contrast to nickel in the IWNi samples, and the metal particle sizes of the $ENi_{NH_3}/500$ samples are slightly larger than those of IWNi.

One may wonder why the nature of the nickel nuclei differs with the preparation conditions. First of all, it is known that nickel and silica possess a strong affinity for each other and very easily form phyllosilicates. For example, the latter may be obtained from nickel hydroxide in a sealed pyrex tube (135–275 °C).[56] They may be also obtained under hydrothermal conditions[52] or at lower temperature and atmospheric pressure during the preparation of Ni/SiO_2 (i) in basic medium,[22,55] (ii) by deposition–precipitation (90 °C, basic medium),[57] and (iii) by hexaamminenickel(II) exchange (25 °C, basic medium).[35,38] It may be noted that, in the case of the preparation by impregnation–washing, the phyllosilicate is formed during drying[42] and not during impregnation since the solution of nickel nitrate is acidic. The phyllosilicates remain stable even after calcination at 500 °C.[51]

In the case of the preparation by exchange with tris(ethylenediamine)nickel(II) in basic solution, grafted nickel is formed instead of phyllosilicate. This may be explained as follows. The coordination of Ni^{II} by ethylenediamine in aqueous medium is thermodynamically favored because of the chelate effect.[58] Complexes with chelate rings are more stable than those containing monodentate ligands such as water or NH_3. The free enthalpy change $\Delta G°$ of the reaction of chelation is negative mainly for entropic reasons because it takes only three en molecules to displace six H_2O or six NH_3 molecules:

$$[Ni(H_2O)_6]^{2+} + 3en \rightleftharpoons [Ni(en)_3]^{2+} + 6H_2O \qquad \log K = 18.02$$

$$4 \text{ mol} \rightleftharpoons 7 \text{ mol}$$

$$[Ni(H_2O)_6]^{2+} + 6NH_3 \rightleftharpoons [Ni(NH_3)_6]^{2+} + 6H_2O \qquad \log K = 8.61$$

It is deduced that $[Ni(en)_3]^{2+}$ with three chelate rings is $\sim 10^{10}$ times more stable than $[Ni(NH_3)_6]^{2+}$.

The enhanced stability of chelated complexes suggests that the ethylenediamine chelating ligands protect the nickel cation and inhibit its reaction with silica. In contrast, when the nickel cation is surrounded by monodentate ligands such as H_2O or NH_3 as in the case of the preparation by hexaamminenickel(II) exchange or by impregnation–washing, it can react with silica to form phyllosilicates. More detailed studies[35,38,50] have shown that, during exchange and also after drying, the $[Ni(en)_3]^{2+}$ complex is in pure electrostatic interaction with silica. During calcination at 300 °C, grafting with silica occurs[59]; at higher temperature, i.e. 600 °C, ethylenediamine ligands are completely removed, leading to the formation of grafted species similar to those in Figure 6.

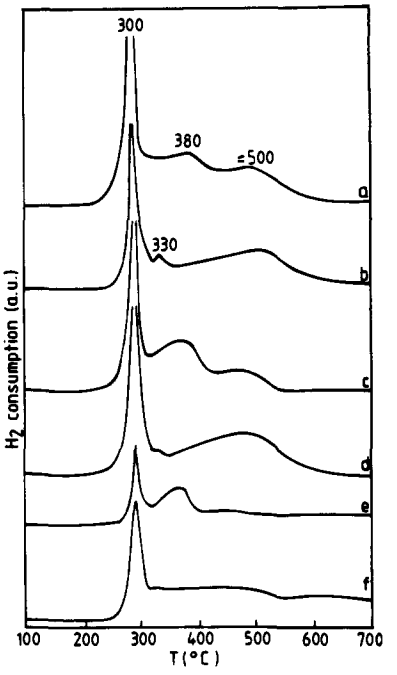

Figure 7. TPR profiles of impregnated samples containing nickel nuclei (a) IWNi5.1+INi9.5, (b) IWNi5.1+INi3.5, (c) ENi_{en}2.4/600+INi6, (d) ENi_{en}2.4/600+INi1.5, (e) ENi_{NH_3}2.7/500+INi3.0, and (f) ENi_{NH_3}2.7/500+INi1.5.

(3) Evidence for Particle Growth When Nickel Is Impregnated on Silica Containing "Nickel Nuclei". As described in the Experimental Section, a "nickel reservoir" was deposited by incipient wetness impregnation on the samples containing "nickel nuclei" characterized above.

The TPR profiles of some of these samples are presented in Figure 7. When the amount of "nickel nuclei" is low compared to that of impregnated nickel (Figure 7a,c,e), the TPR profile is rather similar to that of the reference samples (Figure 3a), i.e. the peak at 380 °C is more intense than the one at 500 °C. In contrast, when the amount of "nickel nuclei" is higher than that of impregnated nickel (Figure 7b,d), the TPR profile is different: the intensity of the peak at 380 °C is weaker than that of the peak at about 500 °C, indicating that nickel becomes less reducible owing to the presence of "nuclei". The peak at 380 °C of the ENi_{NH_3}2.7/500+INi1.5 sample is even absent (Figure 7f). A new weak peak at 330 °C is also visible. It may be noted that, in contrast to the IWNi+INi and ENi_{en}/600+INi samples, nickel of the ENi_{NH_3}/500+INi samples is not completely reduced at 700 °C (Figure 7e,f), as for the ENi_{NH_3}/500 samples (Figure 3b).

After TPR up to 700 °C, the particle size distribution, the average size, and the concentration of particles were measured for each type of samples (Table 3) and compared to those of reference samples (Table 2) and samples containing "nickel nuclei" only (Table 3).

The experimental results shown in Table 3, and Figure 8 and 9, lead to the following remarks:

(1) The metal particle sizes of the samples prepared by the two-step procedure are more homogeneous and smaller than

(54) Carriat, J. Y.; Che, M.; Kermarec, M.; Decarreau, A. *Catal. Lett.* **1994**, *25*, 127–140.

(55) Clause, O.; Bonneviot, L.; Che, M.; Dexpert, H. *J. Catal.* **1991**, *130*, 21–28.

(56) Longuet, J. *C. R. Acad. Sci. Paris* **1947**, *225*, 869–872.

(57) Hermans, L. A. M.; Geus, J. W. *Preparation of Catalysts III*; Poncelet, G., Grange, P., Jacobs, P. A., Eds.; Elsevier: Amsterdam, 1983; pp 113–129.

(58) Cotton, F. A.; Wilkinson, G. W. *Advanced Inorganic Chemistry*, 3rd ed.; Interscience Publishers, John Wiley & Sons: New York, 1972; pp 650-652.

(59) Bonneviot, L.; Clause, O.; Che, M.; Manceau, A.; Dexpert, H. *Catal. Today* **1989**, *6*, 39–46.

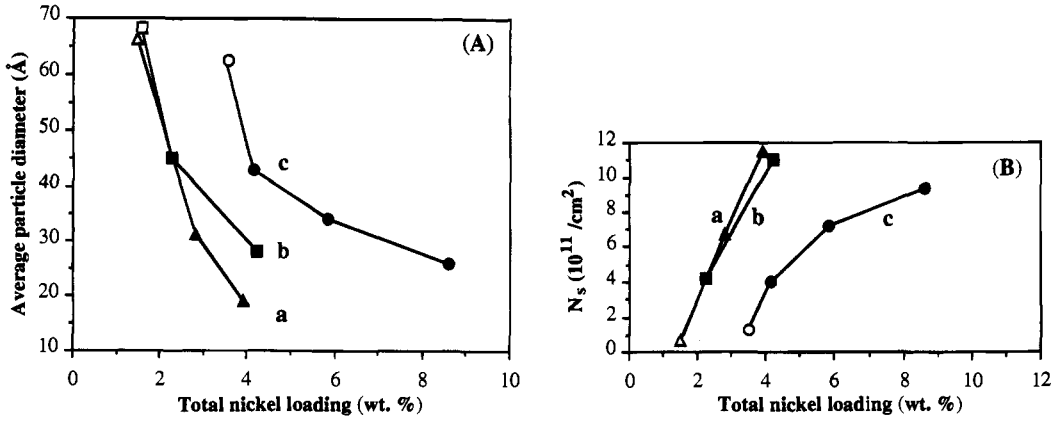

Figure 8. Average diameter of metal particles (A) and number of metal particles per surface unit (N_s) (B) versus the total nickel loading for a given amount of impregnated nickel and an increasing loading in nickel nuclei: (**a**, ▲) impregnated INi1.5 on nickel nuclei ENi$_{en}$/600, (△) INi1.5; (**b**, ■) impregnated INi1.5 on nickel nuclei ENi$_{NH_3}$/500, (□) INi1.5; (**c**, ●) impregnated INi3.5 on nickel nuclei IWNi, (○) INi3.5.

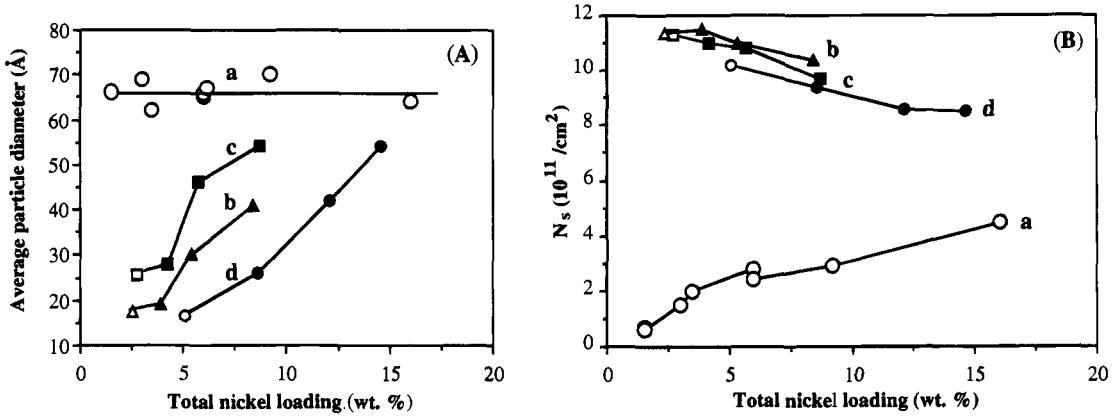

Figure 9. Average diameter of metal particles (A) and number of metal particles per surface unit (N_s) (B) versus the total nickel loading for a given amount of nickel nuclei and an increasing loading in impregnated nickel: (**a**, ○) reference: impregnated INi samples; (**b**, ▲) impregnated INi on nickel nuclei ENi$_{en}$2.4/600, (△) ENi$_{en}$2.4/600; (**c**, ■) impregnated INi on nickel nuclei ENi$_{NH_3}$2.7/500, (□) ENi$_{NH_3}$2.7/500; (**d**, ●) impregnated INi on nickel nuclei IW5.1, (○) IWNi5.1.

those of the reference samples (Table 3); their average diameter lies between that of metal particles made from the reduction of reference samples (68 Å) and of those made from "nickel nuclei"-containing samples (18 Å).

(2) The average particle size decreases when the number of "nickel nuclei" increases for a given amount of impregnated nickel regardless of the method used for the preparation of "nickel nuclei" (Figure 8A). At the same time, the size distribution becomes narrower (Table 3) and the concentration of metal particles (N_s) increases (Figure 8B).

(3) The average particle size increases when the amount of impregnated nickel increases for a fixed amount of "nickel nuclei" (Figure 9A), and the size distribution becomes broader (Table 3). In addition, N_s slightly decreases (Figure 9Bb,c,d), in contrast with that of the reference samples, which increases when the nickel loading increases (Figure 9Ba).

(4) The particle size distribution of these samples prepared in two steps (Figure 10a) is obviously not the weighted summation of those originating from samples with "nickel nuclei" (Figure 10b) and impregnated nickel (Figure 10c).

It is clear that the average particle size is smaller than that of reference samples, that the size distribution is narrower, and that N_s does not increase after impregnation. These results suggest that the growth occurs from impregnated nickel on the "nickel nuclei", regardless of the method of preparation of the latter. The results also show that the nickel in strong interaction with silica really acts as nucleation sites and that the impregnated nickel acts as a "reservoir" for the particle growth and does not contribute to any appreciable extent to the creation of new particles. In consequence, the results suggest that the formation of nickel particles on the silica support takes place via a mechanism of nucleation and growth.

The nickel particles arising from the reduction of the ENi$_{en}$/600 samples whose nickel is grafted, i.e. in extraframework position, are smaller than those of ENi$_{NH_3}$/500 and IWNi, whose nickel is in phyllosilicates, i.e. in the framework position; the ENi$_{en}$/600 samples also lead to the formation of the smaller particles after impregnation and reduction (Table 3). Therefore, the size of the metal nickel particles resulting from the two-step preparation does not only depend on the relative amounts of "nickel nuclei" and of impregnated nickel but also on the nature of the "nickel nuclei".

In consequence, it appears possible to control the nickel particle size between 20 and 60 Å owing to the nickel loading deposited at each preparation step and the method chosen for the preparation of "nickel nuclei".

It must be mentioned that the average particle size (Figure 9A) increases roughly linearly with the weight loading of impregnated nickel and not as the cubic root as expected for spherical or hemispherical particles. The difference may be due to several factors:

(1) The concentration of metal particles (N_s) after impregnation is slightly lower than that of the "nickel nuclei", and all the more as the loading of impregnated nickel is high (Figure 9B). This result indicates that there is probably also particle coalescence during the growth process.

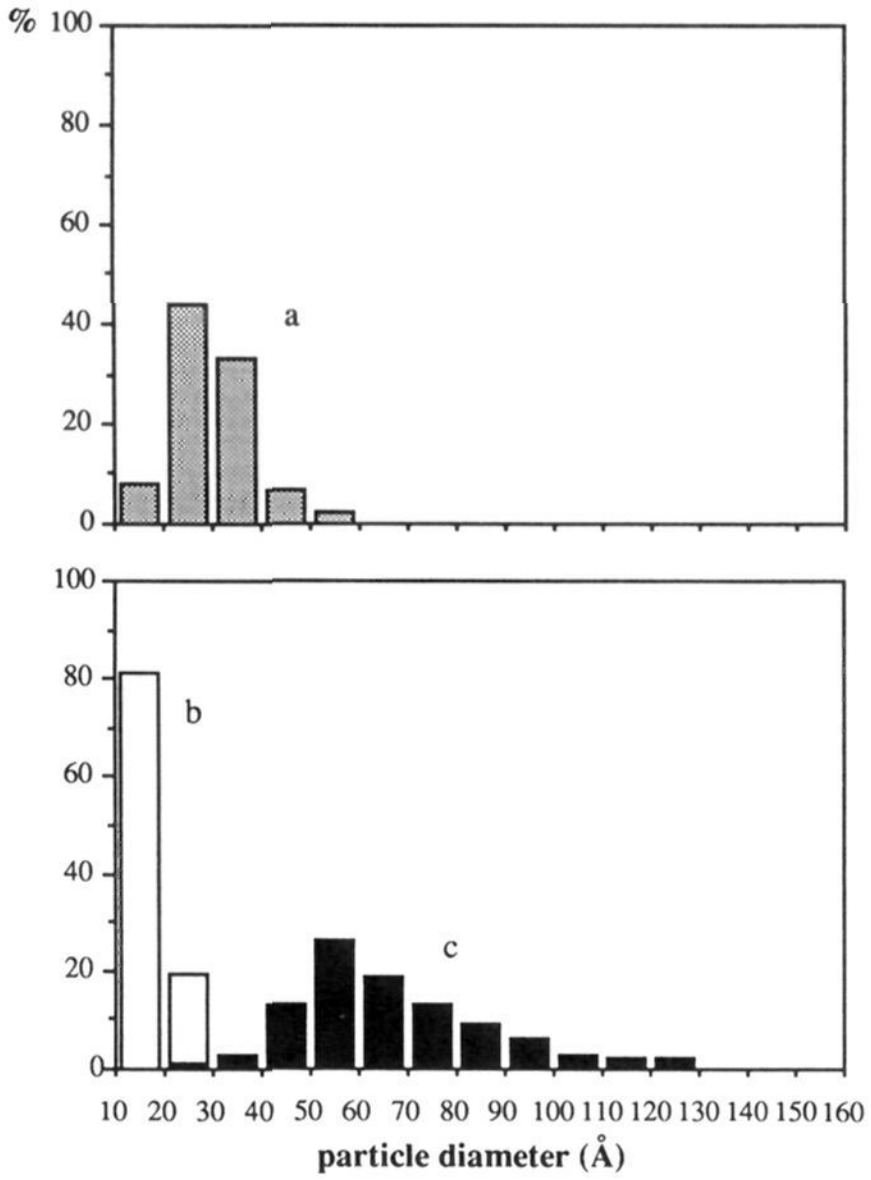

Figure 10. Particle size distribution of the nickel particles obtained after reduction by TPR up to 700 °C: (a) $ENi_{en}2.4/600+INi3$, (b) $ENi_{en}2.4/600$, and (c) INi3.

(2) The particle shape may not be spherical. For raft particles, the size should increase as the square root of the Ni loading. However, there is no such evidence.

(3) The measurement of the particle size from the electron micrographs is not very accurate although the variations of the average particle sizes are meaningful. Indeed, the detection limit for the TEM measurement of nickel metal particles supported on silica is about 10 Å and the contrast of the particles over the silica support is poor. In consequence, the smaller particles may probably not all be counted.

In consequence, the changes in particle size measured via electron micrographs are real although the absolute values have to be considered with caution. Other methods such as hydrogen chemisorption or magnetic measurements could have been used. However, electron microscopy is the only technique which provides direct information on particle size, size distribution, and particle concentrations, in contrast to those other methods.

The metal particle size also depends on the reduction conditions and may be affected by other experimental conditions. For example, increasing the gas flow rate or decreasing the temperature ramp would probably lead to completely reduced particles at 700 °C in the $ENi_{NH_3}/500+INi$ samples.

(4) Determination of the Step At Which Particle Growth Occurs. By analogy with the mechanisms of nucleation and growth of metal thin film or metal powder,[60] it was tempting to believe that the nickel particle growth occurs during nickel reduction. This hypothesis implies that before reduction the "nickel nuclei" and the "nickel reservoir" are separated from each other over the silica surface and that during TPR the Ni^0

(60) Davis, S. C.; Klabunde, K. *Chem. Rev.* **1982**, *82*, 153−208.

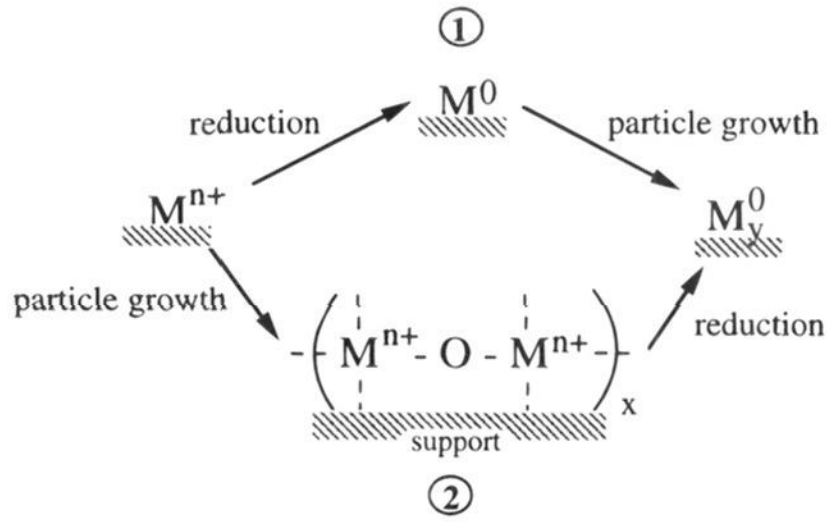

Figure 11. Scheme of two possible ways for the particle growth onto nuclei.

metal atoms issued from the "reservoir" would migrate onto the "nickel nuclei" (pathway 1 of Figure 11).

In a previous study on the characterization of impregnated Ni/SiO_2 materials,[42] we have established that during TPR the NiO particles arising from the decomposition of nickel nitrate at 320 °C are reduced into Ni^0 at 400 °C without any nickel migration. Between 400 and 700 °C, the weak increase observed in the Ni^0 particle size is due to the reduction of nickel phyllosilicates and possibly to some Ni^0 migration. In other words, in impregnated samples, the metal particle size is mainly determined by that of its Ni^{II} oxide precursor. This was also observed by Tohji et al.,[61] who claimed that the reason the nickel metal particle size distribution depends on the Ni/SiO_2 preparation procedure is ascribed to whether or not an homogeneous dispersion of small metal oxide cluster is obtained before reduction. Hence, it would be not surprising that, in the present work, the growth of the particle on the "nickel nuclei" could take place before reduction (pathway 2 of Figure 11).

(a) Particle Growth on "Nickel Nuclei" in the Oxidized State Ni^{II}. It may be noted that, when nickel is impregnated on samples containing "nuclei", the less intense the TPR peak at 380 °C, the smaller the average particle size. Indeed, the samples $IWNi5.1+INi3.5$, $ENi_{en}2.4/600+INi1.5$, and $ENi_{NH_3}2.7/500+INi1.5$, which possess the smallest particles, 26, 26, and 28 Å, respectively (Table 3), exhibit TPR profiles without any peak at 380 °C (Figure 7b,d,f). In order to determine whether the particle growth occurs when nickel is in the oxidized state Ni^{II}, these three samples as well as the $en-SiO_2+INi1.5$ reference sample were characterized after interruption of the TPR at 320 °C, i.e. after nitrate decomposition and before nickel reduction. At this point, the sizes of the NiO particles characterized by microdiffraction lie in the range 20−140 Å for the reference sample, whereas they are smaller than 30 Å for the $IWNi5.1+INi3.5$ sample and not visible for the other two (Table 4). Hence, nickel impregnated on silica containing "nickel nuclei" gives much smaller NiO particles than nickel impregnated on silica. These small NiO particles probably anchored on the "nickel nuclei" are more difficult to reduce, as attested by the small TPR peak at 380 °C (Figure 7b,d,f), than NiO of the reference samples (Figure 3a). It may be deduced that the particle growth occurs before the formation of NiO, i.e. before the TPR temperature of 320 °C is reached. The question now arises as to whether it takes place either at the beginning of the TPR, during sample drying at 90 °C, or during impregnation.

Table 4 also shows that the reduction of these samples between 400 and 700 °C induces an increase in the metal particle

(61) Tohji, K.; Udagawa, Y.; Tanabe, S.; Ueno, A. *J. Am. Chem. Soc.* **1984**, *106*, 612−617.

Table 4. Characteristics of the Nickel Particles Obtained during TPR in Impregnated Samples Containing Nickel Nuclei and in Reference Samples

samples	NiO particle size after TPR up to 320 °C	Ni^0 particle size after TPR up to 400 °C	Ni^0 particle size after TPR up to 700 °C
$ENi_{NH_3}2.7/500+INi1.5$	nonvisible	10−30 Å (100%)[a]	10−30 Å (75%)
$ENi_{en}2.4/600+INi1.5$	nonvisible	10−20 Å (100%)	10−20 Å (77%)
IWNi5.1+INi3.5	10−30 Å (100%)	10−30 Å (100%)	10−30 Å (85%)
ref: en−SiO_2/600+INi1.5	20−140 Å (100%)	20−100 Å (100%)	20−100 Å (90%)

[a] Percentage of particles within the given range of size.

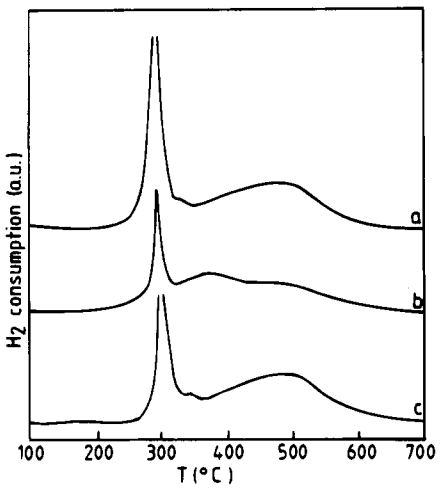

Figure 12. TPR profiles of $ENi_{en}2.4/600+INi1.5$: (a) dried at 90 °C, (b) dried at 25 °C during 24 h, and (c) as in b then dried at 90 °C for 24 h.

Table 5. Influence of the Drying Temperature on the Particle Size

samples	drying temperature (°C)/24 h	$\bar{d}$ (Å)	size dist (Å)
ref: INi	25 or 90	65	20−150
IWNi5.1+INi3.5	90	26	10−50
IWNi5.1+INi3.5	25	38	10−100
IWNi5.1+INi3.5	25 then 90	28	10−50
$ENi_{NH_3}2.7/500+INi1.5$	90	28	10−80
$ENi_{NH_3}2.7/500+INi1.5$	25	40	10−130
$ENi_{NH_3}2.7/500+INi1.5$	25 then 90	28	10−80
$ENi_{en}2.4/500+INi1.5$	90	19	10−40
$ENi_{en}2.4/500+INi1.5$	25	39	10−120
$ENi_{en}2.4/500+INi1.5$	25 then 90	20	10−40

size, probably due to Ni^0 migration. However, less than 25% of the particles reduced at 700 °C are larger than those reduced at 400 °C, confirming that metal nickel migration is not the main mechanism for the particle growth.

(b) Influence of the Drying Temperature on the Particle Growth. Part of the IWNi5.1+INi3.5, $ENi_{en}2.4/600+INi1.5$, and $ENi_{NH_3}2.7/500+INi1.5$ samples were dried in air for 24 h at 25 °C instead of 90 °C. The corresponding TPR profiles exhibit a more intense peak at 380 °C (Figure 12b) than after drying at 90 °C (Figure 12a). In addition, the particle size distribution after TPR up to 700 °C is broader and the average particle size larger (Table 5) than for samples dried at 90 °C. However, they remain respectively narrower and smaller than for reference samples (Table 2). After drying at 25 °C, part of the samples were dried further at 90 °C for 24 h. The TPR profiles and particle sizes are identical to the samples directly dried at 90 °C (Figure 12a,c, Table 5).

These results show the drastic influence of the drying temperature on the particle size. It was shown in ref 42 that the drying temperature has no influence on the particle size of nickel impregnated on silica. Therefore, it may be deduced that the effect of the temperature described here is related to the presence of "nickel nuclei" on silica.

Hence, the particle growth onto "nickel nuclei" appears to be more efficient for samples dried at 90 °C than at 25 °C, suggesting that it occurs during the drying step at 90 °C rather than during impregnation or during the beginning of the TPR.

(5) Mechanism of Particle Growth. The last question concerns the particle growth mechanism. We have shown earlier[42] that, during the drying step of impregnated nickel, nickel nitrate was transformed into basic nickel nitrate $Ni(NO_3)_2{\cdot}2Ni(OH)_2$. This compound, hereafter called $HO-Ni^{II}_{imp}$, contains OH groups. The "nickel nuclei" in $ENi_{NH_3}/500$ or IWNi which belong to phyllosilicates also possess OH groups and are hereafter referred to as $Si-O-Ni^{II}_N-OH$, where N stands for nuclei. The grafted nickel in $ENi_{en}/600$ samples exhibits water molecules in its coordination sphere (Figure 6); it is abbreviated as $Si-O-Ni^{II}_N-OH_2$. It is proposed that when impregnated nickel on silica containing "nickel nuclei" is dried at 90 °C, basic nickel nitrate is formed whose OH groups can condense with the coordinated H_2O of the grafted nickel:

$$Si-O-Ni^{II}_N-OH_2 + HO-Ni^{II}_{imp} \rightarrow Si-O-Ni^{II}_N-\overset{H}{O}-Ni^{II}_{imp} + H_2O \quad (I)$$

or with the OH groups of the nickel phyllosilicates:

$$Si-O-Ni^{II}_N-OH + HO-Ni^{II}_{imp} \rightarrow Si-O-Ni^{II}_N-O-Ni^{II}_{imp} + H_2O \quad (II)$$

These reactions are analogous to those of olation and oxolation taking place during metal ion polymerization in sol−gel processes.[62,63] It may be noted that Che et al.[29,64] have also proposed an olation reaction to explain the phenomenon of nucleation and growth of nickel hydroxides onto silica during the preparation of Ni/SiO_2 materials by deposition−precipitation.

When the samples are dried at 25 °C instead of 90 °C, nickel nitrate is not transformed into basic nickel nitrate,[42] so that reactions I and II cannot take place. However, nickel nitrate may afterward partially be transformed at the beginning of the TPR, before its decomposition into NiO at 300 °C. However, the duration of the TPR between 25 and 320 °C is probably too short to allow the formation of enough basic nitrate to react with the "nickel nuclei", so as to lead to an homogeneous growth of particles and therefore the formation of small particles.

This growth mechanism of nickel particles in an oxidized state is different from the growth mechanisms known in other systems:

(1) During metal vapor condensation on a monocrystalline oxide, once the nuclei are formed, a stage which is not yet well

(62) Livage, J.; Henry, M.; Sanchez, C. *Prog. Solid State Chem.* **1988**, *18*, 259−341.
(63) Brinker, C. J.; Scherer G. W. *Sol-Gel Science: the Physics and Chemistry of Sol-Gel Processing*; Academic Press: San Diego, CA, 1990; pp 26−28.
(64) Che, M.; Bonneviot, L. *Successful Design of Catalysts*; Inui, T., Ed.; Elsevier: Amsterdam, 1988; pp 147−158.

documented but which probably occurs when the first atoms reach the surface,[65] the particle growth on nuclei occurs in the metallic state. It proceeds via metal migration on the support surface or by capture of gaseous metal atoms by the particles.[60,66]

(2) During the preparation by exchange of Pt, Pd, or Ni metal complexes in NaY zeolites, followed by calcination and reduction, Homeyer and Sachtler[13] have shown that the particle growth is an intricate phenomenon. Depending on the conditions of calcination and reduction and on the location of the "nickel nuclei", which are always metal clusters in contrast to our samples, the particle growth may occur with a "reservoir" in oxidized or reduced state.

(3) During solvated metal atom dispersion on an oxide support, it was shown[8] for example that toluene-solvated cobalt atoms nucleate at surface OH groups and the resultant cobalt oxide surface species serve as sites for nucleation of more cobalt atoms, leading to very small, reactive metallic particles.

Conclusion

Ni/SiO_2 materials were prepared with a two-step procedure. Step 1: Formation of "nickel nuclei", i.e. of nickel in strong interaction with silica. They were obtained either by (i) ion-exchange with hexaamminenickel(II) followed by calcination at 500 °C ($ENi_{NH_3}/500$ samples):

$$[Ni(NH_3)_6]^{2+} + \text{silica} \xrightarrow[500\ ^\circ C]{\text{calcination}} \text{2:1 nickel phyllosilicate}$$

(ii) ion-exchange with tris(ethylenediamine)nickel(II) followed by calcination at 600 °C ($ENi_{en}/600$ samples):

$$[Ni(en)_3]^{2+} + \text{silica} \xrightarrow{\text{calcination/600 °C}} \text{grafted nickel}$$

or (iii) by impregnation−washing (IWNi samples):

$$Ni(NO_3)_2{\cdot}6H_2O + \text{silica} \xrightarrow[\text{then washing}]{\text{drying/90 °C,}} \text{1:1 nickel phyllosilicate}$$

Step 2: Deposition of the "nickel reservoir", i.e. nickel in weak interaction with silica by nickel impregnation onto silica containing "nickel nuclei":

$$Ni(NO_3)_2{\cdot}6H_2O + \text{"nickel nuclei" onto silica then drying/90 °C}$$

After TPR up to 700 °C, the nickel metal particles are smaller and the size distribution is narrower than the corresponding ones obtained by single impregnation on silica. The surface concentration of particles (N_s) is found to be close to that of the "nickel nuclei".

Noteworthy is the fact that the particle size depends on the respective amounts of nickel deposited at each step of preparation. For a given amount of the "nickel nuclei" and an increasing amount of impregnated nickel, the average particle size increases while the particle concentration does not. For a given amount of impregnated nickel and an increasing amount of "nickel nuclei", the particle concentration increases and the average particle size decreases. The latter result means that it is possible to obtain decreasing metal particle size although the total Ni loading (Ni nuclei + impregnated Ni) increases. These results suggest that impregnated nickel grows up on "nickel nuclei" and that a mechanism of nucleation and growth is involved in the two-step preparation.

The particle growth on "nickel nuclei" takes place after impregnation during the drying step of the samples at 90 °C, i.e. when nickel is still in the Ni^{II} oxidation state. At 90 °C, nickel nitrate of the impregnated nickel is decomposed into basic nitrate containing hydroxyl groups. The growth mechanism probably occurs via a condensation reaction between these hydroxyl groups and either those contained in phyllosilicates which constitute the "nickel nuclei" in IWNi and $ENi_{NH_3}/500$ samples or water coordinated to grafted nickel of the "nickel nuclei" in $ENi_{en}/600$ samples.

The present work shows that, for the Ni/SiO_2 system, it is possible to obtain metal particles with a rather narrow distribution and an average size which can vary from 20 to 60 Å, depending on the choice of the method of preparation of "nickel nuclei" and on the amount of nickel involved at each step. Further work is in progress to check whether the same principles apply for other transition metal−oxide support couples.

JA9339357

(65) A possible reaction between Ni^0 and the support would be

$$Ni^0 + 2HOSi{\equiv} \rightharpoonup Ni^{II}(OSi{\equiv})_2 + H_2$$

according to ref 6b and to the following: Martino, G. *Growth and Properties of Metal Clusters*; Bourdon, J., Ed.; Elsevier: Amsterdam, 1980; pp 399−413.

(66) Masson, A. *Contribution of Cluster Physics to Materials Science and Technology*; Davenas, J., Rabette, P. M., Eds.; Martinus Nijhoff Publishers: Dordrecht, The Netherlands, 1986; pp 295−309.